Rev.Adv.Mater.Sci. 18(2008) 590-592

DIFFERENT NANOCRYSTALLIZATION SEQUENCE DURING HIGH PRESSURE TORSION AND THERMAL TREATMENTS OF AMORPHOUS $Cu_{60}Zr_{20}Ti_{20}$ ALLOY

S. Hóbor[1], Á. Révész[1,2], A. P. Zhilyaev[3] and Zs. Kovács[1]

[1]Dept. Materials Physics, Eötvös University, Budapest, H-1518, P.O.B. 32, Budapest, Hungary
[2]Dept. Physics, University of Maryland, Baltimore County, 1000 Hilltop Circle, Baltimore, MD 21250, USA
[3]Institute for Metals Superplasticity Problems, RAS, 39 Khalturin St., Ufa, 450001, Russia

Received: March 29, 2008

Abstract. Nanocrystallization behavior of $Cu_{60}Zr_{20}Ti_{20}$ amorphous ribbon induced by severe plastic deformation and by linear heating thermal treatment has been compared. Thermal treatment of the as-quenched ribbon results in the joint formation of two crystalline phases, on contrary, plastic deformation at room temperature induces the precipitation of only Cu_2ZrTi.

1. INTRODUCTION

Cu-based bulk metallic glasses (BMGs) with high glass forming ability were obtained in ternary Cu-(Zr or Hf)-Ti systems [1]. These systems exhibit good mechanical properties, e.g. high tensile strength and remarkable plasticity [2]. Recently, room temperature severe plastic deformation induced nanocrystallization, e.g. by cold rolling [3] and high pressure torsion (HPT) [4-5] has received increased attention. During the HPT processing, a porosity and impurity-free disc-shaped sample is strained by torsion under high pressure [6]. Generally, the deformation induced nanocrystals are localized in shear bands, where the atomic mobility is enhanced and the local structure of the amorphous alloy can change [7].

In the present work, the nanocrystal formation in $Cu_{60}Zr_{20}Ti_{20}$ amorphous ribbon subjected to the HPT technique has been analyzed and compared to the rapidly quenched amorphous alloy.

2. EXPERIMENTAL

An ingot of nominal composition of $Cu_{60}Zr_{20}Ti_{20}$ was prepared by induction melting of high purity (99.9%) Cu, Zr and Ti metals. Ribbons were obtained by using single roller melt spinning technique in inert atmosphere with a Cu-wheel rotating at a tangential velocity of 3800 rpm. The fully amorphous ribbons have been cut into flakes and then placed between HPT anvils and compressed into several discs with a diameter of 8 mm and thickness of about 120 mm under an applied pressure of 6 GPa with 5 whole turns. Due to the asymmetry of the deformation the plunger and the support sides of the HPT disc are distinguished and will be denoted as Side 1 and Side 2.

Corresponding author: S. Hobor, e-mail: hobors@metal.elte.hu

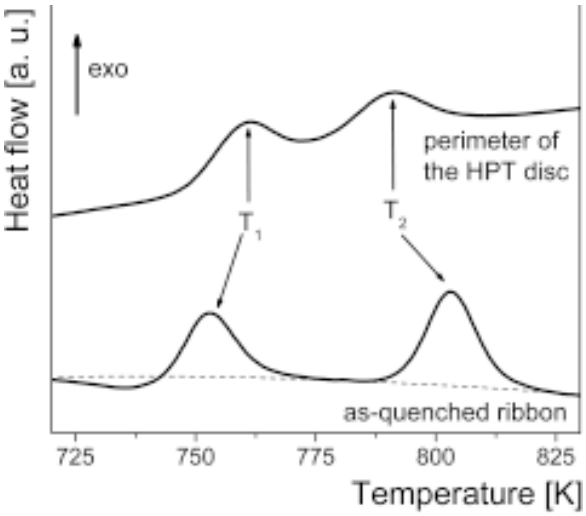

Fig. 1. DSC curves of the as-quenched $Cu_{60}Zr_{20}Ti_{20}$ ribbon and the perimeter of the HPT disc obtained at 40 $Kmin^{-1}$ heating rate.

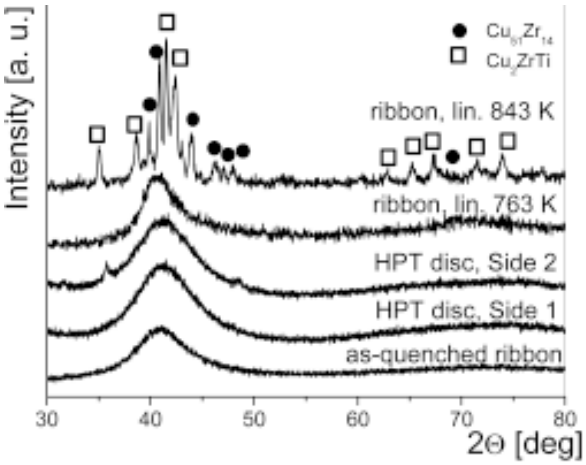

Fig. 2. XRD patterns corresponding to the as-quenched $Cu_{60}Zr_{20}Ti_{20}$ ribbon, the support (Side S) and the plunger (Side P) sides of the HPT disc and heat treated ribbon samples above the first (763K) and the second (843K) crystallization stages.

Microstructures were examined by powder X-ray diffraction (XRD) on a Philips Xpert diffractometer using CuK_α radiation in θ-2θ geometry.

A Perkin Elmer power compensated differential scanning calorimeter (DSC) was used to investigate the thermal behavior and crystallization applying continuous heating experiments performed at scan rate of 40 K/min.

3. RESULTS AND DISCUSSION

Continuous heating DSC curves corresponding to the as-quenched ribbon and to the severely deformed HPT disc are plotted in Fig 1. Practically, both signals show similar features: a glass transition is followed by two sharp exothermic peaks (T_1, T_2) corresponding to a two-stage crystallization process. Severe plastic deformation results in a less pronounced glass transition, a drop of T_2 and a shift of T_1 to higher temperatures, indicating a higher thermal stability.

Fig. 2 summarizes the XRD investigations on the different states of the amorphous $Cu_{60}Zr_{20}Ti_{20}$ alloy. The as-quenched ribbon and the two sides of the HPT disc (Side 1 and Side 2) show a broad symmetric halo at around 2Θ=41 deg, however, the pattern corresponding to Side 2 exhibits faint crystalline peaks at around 2Θ=32, 36, 48 deg corresponding to the formation of crystalline blocks embedded in the amorphous matrix. The spectrum of the sample heated above the first crystallization stage (763K) shows a more asymmetric halo, while the pattern taken after the second peak (843K) changes drastically and indicates the decomposition of the amorphous alloy into hexagonal $Cu_{51}Zr_{14}$ (a=1.13 nm, c=0.824 nm) and hexagonal Cu_2ZrTi (a=0.514 nm, c=0.823 nm) phases [8]. The XRD peak positions of Side 2 of the HPT disc are clearly different from those of the hexagonal phases obtained after the second stage, however, can be fitted by a hexagonal phase with lattice parameters of a=0.492±0.002 nm and c=0.8±0.003 nm.

In-situ synchrotron [9] and other in-situ XRD measurements [10] have shown that thermal activation during both linear heating and isothermal annealing first promotes the precipitation of $Cu_{51}Zr_{14}$ phase from the amorphous $Cu_{60}Zr_{20}Ti_{20}$ matrix which is then followed by the formation of Cu_2ZrTi phase. In contrast, the room temperature HPT-deformation of the amorphous alloy leads to the formation of only one hexagonal phase (see Fig. 2).

4. CONCLUSIONS

High pressure torsion of fully amorphous $Cu_{60}Zr_{20}Ti_{20}$ alloy promotes the formation of

nanocrystals embedded in the amorphous matrix. The precipitation of only hexagonal Cu_2ZrTi crystallites during severe plastic deformation supports the existence of a different crystallization sequence compared to thermal annealing.

ACKNOWLEDGEMENTS

The authors gratefully acknowledge the support of INTAS 03-51-3779 project. The work has been supported by the Hungarian Scientific Research Fund (OTKA) under grants D048461 (Postdoctoral Research Fellowship of Zs. K.) and T-043247. A. R. acknowledges the Hungarian-American Scholarship Enterprise Fund (HAESF) for a Senior Fellowship.

REFERENCES

[1] A. Inoue, W. Zhang, T. Zhang and K. J. Kurosaka // *Acta Mater.* **49** (2001) 2645.
[2] A. Inoue, W. Zhang, T. Zhang and K. J. Kurosaka // *Non-Cryst. Solids* **304** (2002) 200.
[3] R.J. Hebert, J.H. Perepezko, H. Rösner and G. Wilde // *Scripta Mater.* **54** (2006) 25.
[4] N. Boucharat, R. Heber, H. Rösner, R. Valiev and G. Wilde // *Scripta Mater.* **53** (2005) 823.
[5] Zs. Kovács, P. Henits, A.P. Zhilyaev and Á. Révész // *Scripta Mater.* **54** (2006) 1733.
[6] R. Z. Valiev, R. K. Islamgaliev and I. V. Alexandrov // *Prog. Mater. Sci.* **103** (2000) 45.
[7] H. Chen, Y. He, G.J. Shiflet and S.J. Poon // *Nature* **367** (1994) 541.
[8] A. Concustell, Á. Révész, S. Suriñach, L.K. Varga, G. Heunen and M.D. Baró // *J. Mater. Res.* **19** (2004) 505.
[9] Á. Révész, S. Hóbor, P.J. Szabó, A.P. Zhilyaev and Zs. Kovács // *Mater. Sci. Eng. A* **460-461** (2007) 459.
[10] J. Z. Jiang, H. Kato, T. Ohsuna, A. Inoue, K. Saksl, H. Franz and K. Stahl // *Appl. Phys. Lett*. **83** (2003) 3299.